

Correlation Effects and Structural Dynamics in the β -Pyrochlore Superconductor KOs_2O_6

J. Kuneš,^{1,2} T. Jeong,¹ and W.E. Pickett¹

¹*Department of Physics, University of California, One Shields Avenue, Davis CA 95616, USA*

²*Institute of Physics, Academy of Sciences of the Czech Republic,*

Cukrovarnická 10, 162 53 Praha 6, Czech Republic

(Dated: November 12, 2018)

Electronic, magnetic, and dynamical properties of the new superconducting β -pyrochlore KOs_2O_6 and related RbOs_2O_6 and CsOs_2O_6 compounds are calculated and compared with experiment and contrasted with structurally related spinel pyrochlores. The calculated susceptibility Stoner enhancement (110%) and thermal mass enhancement $\lambda = 2.5\text{-}3$ reflect moderate but perhaps important Coulomb correlations. The K^+ ion optic mode is found to be unstable, allowing large excursions of $0.5\text{-}0.6 \text{ \AA}$ from its ideal site of the K ion along $\langle 111 \rangle$ directions. This dynamical mode is much less anharmonic in the isostructural Rb and Cs compounds (with larger cations), perhaps accounting for their progressively lower values of T_c . Electron scattering from this very anharmonic mode may be the cause of the anomalous concave-downward resistivity that is seen only in KOs_2O_6 .

PACS numbers: 74.70.Dd, 74.25.Jb, 74.25.Kc

I. INTRODUCTION

Transition metal oxides with metal ions (T) lying on a pyrochlore sublattice display a wide variety of behavior. In the 1970s LiTi_2O_4 was the anomalous “high T_c ” oxide superconductor amongst intermetallics, with its $T_c = 13\text{K}$. The vanadate LiV_2O_4 became the first (and still essentially the only) true heavy fermion metal based on d electrons rather than f electrons. Considerable theoretical speculation on the microscopic basis for this heavy fermion behavior has left no consensus. Other members of the pyrochlore structure, such as CuIr_2S_4 and $\text{Tl}_2\text{Ru}_2\text{O}_7$, exhibit charge ordering and accompanying structural adjustment, possibly associated with the high symmetry of the undistorted structure. The “pyrochlore” sublattice occupied by the transition metal ions is comprised of corner-sharing tetrahedra that are known to be highly frustrating for nearest neighbor antiferromagnetic (AFM) spin couplings.[1, 2]

Recently Yonezawa *et al.*[3, 4] reported the discovery of a superconductor KOs_2O_6 with a $T_c = 9.6\text{K}$, with β -pyrochlore structure, a new variant of the pyrochlore class, and superconductivity was quickly obtained in isostructural and isoelectronic RbOs_2O_6 (6.3 K)[5] and CsOs_2O_6 (3.2 K)[6] as well, suggesting new physics generic to this structural variant. The other example of superconductivity in $4d/5d$ pyrochlore oxides is $\text{Cd}_2\text{Re}_2\text{O}_7$ with $T_c = 1 \text{ K}$. [7] There is no obvious indication of strong enhancement by correlation effects in the quasiparticle mass for the β -pyrochlore compounds. Using the specific heat jump ΔC at T_c and the weak coupling relation $\Delta C/T_c = 1.43\gamma$, Hiroi *et al.* [4] obtained a linear specific heat coefficient $\gamma = 19 \text{ mJ/K}^2 \text{ mol-Os}$, which is not especially large. The magnitude has been confirmed for RbOs_2O_6 by Brühwiler *et al.* [8] who obtained $\gamma = 17 \text{ mJ/K}^2 \text{ mol-Rb}$ from the heat capacity. However, one highly unusual feature is that, while the re-

sistivity $\rho(T)$ of both RbOs_2O_6 (Ref. [5]) and CsOs_2O_6 (Ref. [6]) have the normal upward curvature at low temperature, KOs_2O_6 with its higher T_c has a very peculiar concave downward shape[4] of $\rho(T)$ immediately above T_c extending to 200 K.

Conventional pyrochlore oxides have the chemical formula $\text{A}_2\text{T}_2\text{O}_7$ or more descriptively $\text{A}_2\text{T}_2\text{O}_6\text{O}'$, where A is a larger cation, T is a smaller transition metal cation, and O' is an oxygen ion in a large tetrahedral site rather than forming the octahedron surrounding the transition metal ion. The distinguishing feature is the T pyrochlore sublattice, a network of corner-sharing tetrahedra that has been widely studied in the context of frustrated antiferromagnetism. Yonezawa *et al.*[3] produced the β variant with the general formula AT_2O_6 where A is a large monovalent alkaline metal cation. KOs_2O_6 has the same space group $Fd\bar{3}m$ as conventional pyrochlore, but the large cations K^+ , Rb^+ , Cs^+ are located (unexpectedly) at the O' site of the conventional pyrochlore structure, thus becoming the $\square_2\text{Os}_2\text{O}_6\text{K}$ variant of conventional pyrochlore (where \square denotes an empty A site). KOs_2O_6 has the lattice constant 10.101 \AA and two formula units per fcc primitive cell.

Although the T ions lie on the same pyrochlore sublattice as in the closely related spinel system AT_2O_4 , and are the centers of TO_6 octahedra, there are *qualitative* differences: in the spinel structure all the *edge-sharing* TO_6 octahedra are aligned along the cubic axes with T atoms being bridged by two O ions, while in the conventional pyrochlore and its β variant there are four different orientations of the *vertex-sharing* TO_6 octahedra and each pair of T ions is bridged by a single O ion. The four different TO_6 octahedra are rhombohedrally distorted along the one of the four cubic body diagonals by an amount determined by the O internal parameter ($u=0.3125$ corresponds to an equilateral octahedron). The pyrochlore lattice of the T sites can be viewed as a 3D generalization of the 2D Kagome lattice (see Fig. 1).

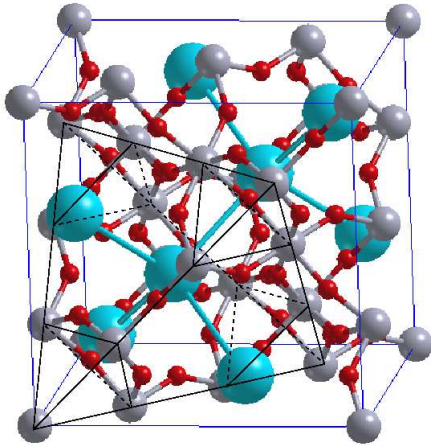


FIG. 1: (color online) The crystal structure of the β -pyrochlore superconductor KOs_2O_6 . The largest atoms are K, the smallest dark spheres are O and are connected by sticks with the midsize atoms, Os. The pyrochlore sublattice formed by Os tetrahedra and truncated-tetrahedral cavities containing K ions is highlighted.

In this paper we initiate the theoretical study of the KOs_2O_6 class of compounds, focusing on the electronic structure in comparison to the well studied conventional pyrochlore and spinel systems. The tight-binding description differs in important ways from the spinel (LiV_2O_4 , say) counterpart, and the density of states $N(E_F)$ at the Fermi level E_F is not high. In fact it is below the average for the t_{2g} band, due to E_F lying in a valley, suggesting either electron or hole doping could enhance T_c by raising $N(E_F)$. We further describe the discovery of an extreme dynamical instability corresponding to displacements of 0.5 \AA or more of the alkali ion along $\langle 111 \rangle$ direction.

II. METHOD

We have used both the full-potential nonorthogonal local-orbital minimum-basis (FPLO) scheme within the local density approximation (LDA)[9] and the full potential linearized augmented plane wave (LAPW) plus local orbitals method as implemented in Wien2k.[10] The exchange and correlation potential of Perdew and Wang[11] was used. In FPLO, K $3s, 3p, 4s, 4p, 3d$ states, Os $4s, 4p, 4d, 4f, 5s, 5p, 6s, 6p$ and O $2s, 2p, 3d$ were included as valence states. The inclusion of the relatively extended $3s, 3p, 4s, 4p, 3d$ semicore states as band states was done because of the considerable overlap of these states on nearest neighbors. The LAPW basis set is

characterized by the atomic sphere radii of 2.05 bohr for K and Os and 1.4 bohr for O, plane-wave cut-off $R_{mt}K_{max}=5.5$ and K- $s, -p$, Os- $s, -p, -f$ and, O- s local orbitals. The self-consistent potentials were calculated using 256 k points in the irreducible zone. The K, Os and O atoms are located at positions $(\frac{3}{8}, \frac{3}{8}, \frac{3}{8})$, $(0, 0, 0)$, and $(u, \frac{1}{8}, \frac{1}{8})$ with site symmetries $\bar{4}3m$, $\bar{3}m$, and $mm2$ respectively. We obtained the internal coordinate $u = 0.317$ by minimizing the total energy with FLAPW method. The corresponding deviation of the O-Os-O bond angle from the right angle is $\pm 1.8^\circ$. Similar u values of 0.316 and 0.315 were obtained for RbOs_2O_6 and CsOs_2O_6 respectively, corresponding to O-Os-O bond angle deviations for right angle of 1.6° and 1.4° . Due to the relaxation of the O-Os-O bond angle the relative differences of Os-O bond lengths are less the relative differences of the lattice constants for the three systems.

III. RESULTS AND DISCUSSION

A. Band and Density of States

The guideline $\text{K}^+\text{Os}_2^{p+}\text{O}_6^{2-}$ leads to the formal valence $p = 5.5$, or a $d^{2.5}$ occupation (out of the six t_{2g} states, including spin). As we see in Fig. 2, this puts E_F within the t_{2g} bands, somewhat below half-filling of the threefold orbitally degenerate complex of bands. Surrounding E_F we have the t_{2g} manifold (as in both pyrochlore $\text{A}_2\text{T}_2\text{O}_7$ and spinel AT_2O_4 systems) of width 3.2 eV (2.9 eV), and above it and separated by 1.6 eV (1.8 eV) is the e_g manifold. The ‘‘O $2p$ bands’’ (with both e_g and t_{2g} character mixed in) are fully occupied and separated from the t_{2g} bands by 0.7 eV (1.5 eV) as shown in Fig. 3 (scalar-relativistic values are shown in the brackets). The non-cubic part of the $\bar{3}m$ crystal field on the Os site is weak and the band structure shows no apparent further splitting of the t_{2g} complex. We show a blowup of the t_{2g} bands around E_F of KOs_2O_6 in Fig. 2. The twelve bands ($3 t_{2g} \times 4$ Os ions) are $5/12$ filled. For comparison we have also calculated the band structures of the other β -pyrochlore superconductors, CsOs_2O_6 and RbOs_2O_6 . The band structures are extremely similar, with the same bandwidth, differing only in fine details.

In Fig. 3 we display the density of states (DOS) of KOs_2O_6 . The calculated Fermi level E_F lies within a valley, giving a value of $N(E_F)=8.3$ states/eV/unit cell (scalar-relativistic value) that is slightly above the average value of 7.5 states/eV in the t_{2g} bands, and E_F lies 0.3 eV above the peak in $N(E)$ arising from the rather flat bands at the bottom of the complex. The DOS plot also indicates that the K states appear nowhere close to the Fermi level and do not exhibit mixing with the Os d states, which limits the role of the alkali ion to a donor of an electron and a source of electrostatic potential (and thus a possible scatterer).

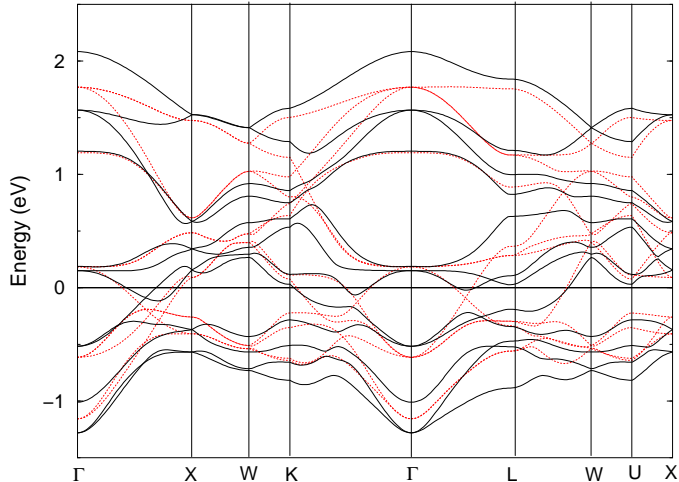


FIG. 2: The Os t_{2g} band complex of the superconductor KOs_2O_6 along fcc symmetry lines. The formal $d^{2.5}$ configuration results in 5/12 filling of these twelve bands. The relativistic bands are marked with full (black) lines, the scalar-relativistic with dotted (red) line.

B. Tight Binding Representation

In order to understand the band structure of the t_{2g} complex, we are thus left to consider the Os lattice bridged by O ions, suggesting a simple tight-binding description. Crystal field splitting reduces the number of relevant orbitals to three t_{2g} states per Os site. Separation of the O bands suggests that the O p states can be “integrated out” and taken into consideration implicitly through the effective Os-Os hopping amplitude. Fujimoto[12] has shown that a single (s) state on a pyrochlore lattice with near neighbor coupling only leads to two dispersing bands and two absolutely flat bands, which reflects the close relation to the Kagome lattice (which has a single flat band). Singh *et al.*[13] considered a much more realistic $dd\sigma, dd\pi$ 12-band model for LiV_2O_4 , and noted that for $dd\pi = \frac{3}{8}dd\sigma$, two of the twelve bands become flat. Unlike for the spinel structure, in the β -pyrochlore structure the principle axes of the t_{2g} states are not aligned with the cubic axes so such a model does not apply directly to KOs_2O_6 .

Based on the geometry of the Os-O-Os bonds we have developed a tight-binding model with three t_{2g} states on four Os sites in the unit cell. In an equilateral octahedron only $dp\pi$ hopping is possible for t_{2g} orbitals (e.g. for O atom at (001) vertex of the local octahedron the $d_{xz} \rightarrow p_x$ and $d_{yz} \rightarrow p_y$ hopping is allowed by symmetry). The effective hopping amplitude between t_{2g} orbitals on neighboring Os sites is then determined by this single parameter and the relative orientation of the corresponding OsO_6 octahedra. This model (see Fig. 4) provides a reasonable band picture except that (1) the order of the T_{2g} and T_{1g} triplets (second and third levels from the bottom of the t_{2g} complex) at the zone center are interchanged

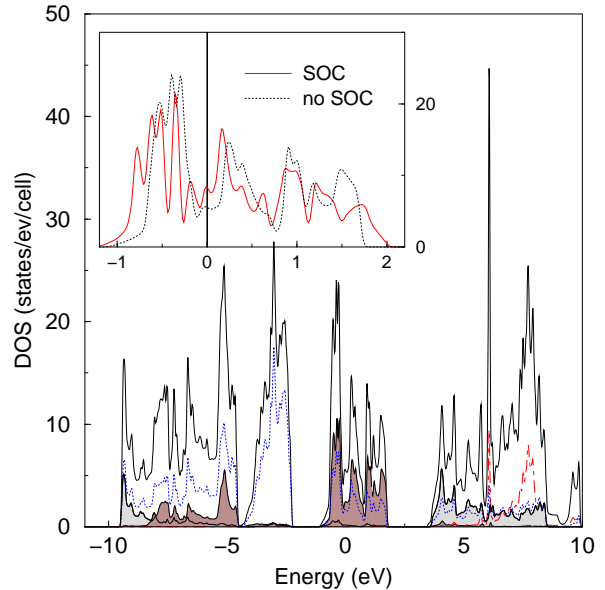


FIG. 3: (color online) Scalar-relativistic density of states (solid line) and the site and orbital projected densities of states of KOs_2O_6 : Os- t_{2g} (dark shading), Os- e_g (light shading), O (dotted line), and K (dot-dashed line). In the inset we show in detail the effect of spin-orbit coupling to the density of states of the t_{2g} manifold.

and thus the band topology in this region (at and below E_F) is incorrect, (2) the four lower bands are too flat, and (3) unphysical degeneracies occur at the zone boundary points X and L (this last point is minor). Inclusion of the coupling to e_g states readily corrects the ordering of the T_{1g} and T_{2g} triplets and thus the band topology as shown in Fig. 4 (right panel). Explicit incorporation of the O $2p$ states into a total 56 band model gives no appreciable change of the Os derived bands, indicating that the O $2p$ bands can be integrated out fairly accurately. The additional dispersion of the flat bands is likely to be due to direct Os-Os hopping. A rough estimate of this effect can be obtained from the Os lattice without O, yielding the d bandwidth less than 1 eV.

C. Fermiology

An appreciable effect of spin-orbit coupling is to be expected in Os $5d$ bands. While the relativistic bands are qualitatively similar to the scalar-relativistic ones, there are some important differences. Removal of some band crossings leads to flatter bands and additional peaks in the density of states. As a result the density of states at the Fermi level is enhanced (see below) and the band structure in the vicinity of Fermi level becomes more sensitive to the oxygen position as we discuss below.

There are two bands crossing the Fermi level in Fig. 2. The first band gives rise to two closed sheets of the Fermi surface centered at the Γ point, which enclose the

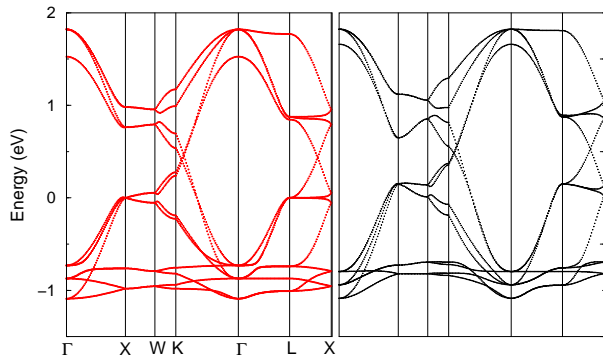


FIG. 4: Tight-binding bandstructure: t_{2g} -to- t_{2g} hopping via oxygen only (left panel), including e_g -to- e_g and e_g -to- t_{2g} hopping (right panel).

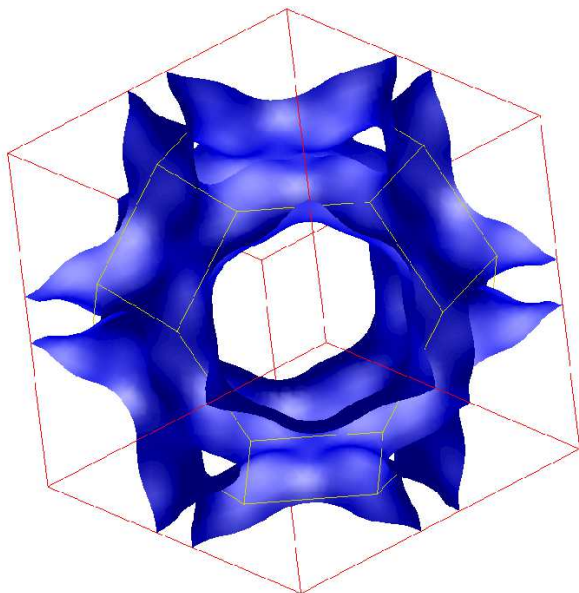


FIG. 5: The connected the Fermi surface with necks along the three-fold axis (spin-orbit coupling included).

electron part of the reciprocal space in between of them (see Fig. 5). The second band leads to a connected Fermi surface with necks along the three-fold axis (see Fig. 6). Visual inspection of the closed sheets of the Fermi surface suggests a possibility of partial nesting, in particular along the $\Gamma - K$ direction. In order to pursue this possibility we have calculated the imaginary part of generalized susceptibility in the low energy limit

$$\text{Im} \chi(\mathbf{q}, \omega) = \pi\omega \sum_{\mathbf{k}} \delta(\epsilon(\mathbf{k}) - E_F) \delta(\epsilon(\mathbf{k} + \mathbf{q}) - E_F) \quad (1)$$

$$= \pi\omega\nu(\mathbf{q}). \quad (2)$$

We emphasize that a large number of k-points is required to get reliable results, see the caption to Fig. 7. The calculated $\text{Im}\chi(\mathbf{q})$ along Γ -K has some sharp Fermi surface related structure, but the peaks are only $\pm 15\%$ from a

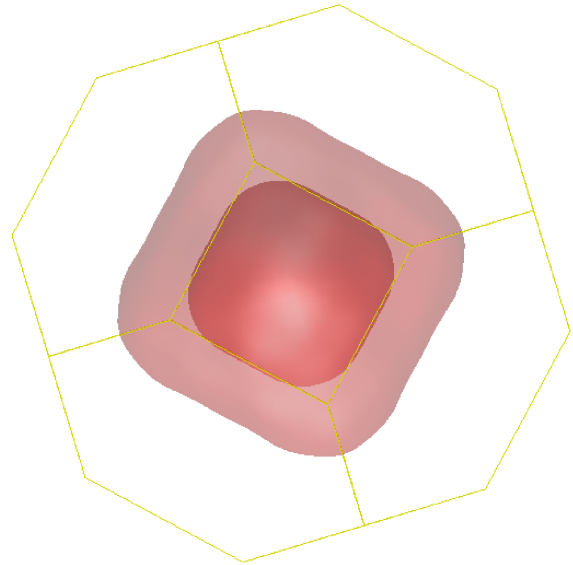


FIG. 6: The closed sheets of the Fermi surface centered on the Γ point (spin-orbit coupling included).

smooth background and so do not suggest electronic instabilities.

For the three β -pyrochlores reported so far (K, Rb, Cs) [3, 5, 6] the transition temperature T_c and the lattice parameter vary inversely as shown in Table I. It is plausible to assume that the structural change is due to the size effect of alkaline metal ions, because the bands near the Fermi level consist of Os 5d orbitals with minor contribution from O 2p orbitals. The decrease of T_c with increasing volume under negative chemical pressure is in contrast to the case of conventional BCS superconductivity in a single band model, where the T_c increases under negative pressure, because the density of states increases (see Table I).

Hiroi *et al.*[4] have inferred the linear specific heat coefficient for KOs_2O_6 of $\gamma=19$ mJ/K² mole-Os from the heat capacity jump at T_c assuming the weak coupling relation $\Delta C/T_c = 1.43\gamma$. A similar value has recently been obtained by Brühwiler *et al.* [8] for RbOs_2O_6 $\gamma=17$ mJ/K² mole-Os directly from the heat capacity. The calculated value of $N(E_F)=28.2$ states/Ry/Os for KOs_2O_6 corresponds to a bare value $\gamma_b=4.9$ mJ/K² mole-Os. The corresponding thermal mass enhancement λ given by

TABLE I: The experimental lattice constants and transition temperatures [3, 5, 6] together with the calculated densities of states at the Fermi level $N(E_F)$ normalized per Os atom and the corresponding unrenormalized linear specific heat coefficient γ_b per mole Os.

Compound	a(Å)	T_c (K)	$N(E_F)$ (Ry ⁻¹)	γ_b (mJ/K ²)
KOs_2O_6	10.101	9.6	28.2	4.9
RbOs_2O_6	10.114	6.3	28.6	5.0
CsOs_2O_6	10.149	3.2	30.3	5.3

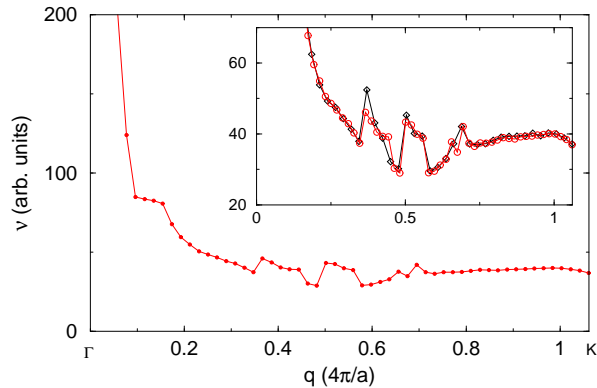


FIG. 7: The low frequency limit of the generalized susceptibility $\nu(\mathbf{q})$ calculated along the Γ -K line obtained with $440 \times 440 \times 440$ k-points (circles) in the cubic Brillouin zone. In the inset we compare with a curve obtained with $160 \times 160 \times 160$ k-mesh (diamonds).

$\gamma/\gamma_b = 1 + \lambda$ gives a large renormalization $\lambda = 2.9$. The value $\lambda = 2.4$ is obtained from the data for RbOs_2O_6 . This renormalization includes the phonon contribution but most likely is due primarily to electronic processes.

Important insight into magnetic fluctuation effects is provided by the enhancement of the bare Pauli susceptibility in a metal. We have evaluated, within the density functional theory formalism, the Stoner enhancement of the susceptibility $\chi = \frac{\chi_0}{(1 - IN(E_F))} \equiv S\chi_0$, where $\chi_0 = 2\mu_B^2 N(E_F)$ is the non-interacting susceptibility and S gives the electron-electron enhancement in terms of the Stoner constant I . We have calculated I using both the Janak-Vosko-Perdew theory [14] and fixed spin moment calculations, obtaining a value of $S = 2.15 \pm 0.05$, which does not indicate any ferromagnetic instability of the paramagnetic groundstate. The spin-orbit coupling was neglected in this calculation.

D. Dynamical Instability

In light of interesting but perhaps limited role of correlation effects (nothing like heavy fermion behavior), we have begun to pursue the character of electron-phonon coupling as a pairing mechanism. Since K^+ is a bare charge in a substantial hole in the β -pyrochlore lattice, we have calculated the energy surface and deformation potential for a K-K “bond stretching” motion of the K ions, which lie on a diamond sublattice (of course, there is no K-K bond, the ions being ionized and also separated by $d_{K-K} = \frac{\sqrt{3}}{4}a = 4.33 \text{ \AA}$). The result we find is a dynamical instability of the K ion. Although the force vanishes by symmetry for the ideal structure, for increasing separation of K ions lying along the $\langle 111 \rangle$ direction the energy decreases. The energy is minimized only after a displacement of the K ion by 0.65 \AA ! This motion is directed along $\langle 111 \rangle$ channels in the Os_2O_6 system, and

this crystal structure may not be stable for the smaller alkali cations Na and Li simply because they do not stay put near the ideal site. In Fig. 8 we show the energy as a function of the alkali ion displacement in this mode for K, Rb and Ce as well as fictitious Na compounds (the lattice constant of KOs_2O_6 was used for the Na compound). Note that the curves are upper bounds, since allowing the Os and O atoms to relax at any displacement would only lower the energy.

The high symmetry position is found to be unstable for Na, while a very flat energy surface is found for K over a large range of displacements. The Rb system exhibits significant anharmonicity, which is reduced when going to Cs. Large differences in the energy surface between systems which have very similar lattice constants and band structures can be understood as follows. If only the effect of the electrostatic potential on the nucleus at the alkali metal site was considered (i.e. if the electron charge was frozen) the site would be dynamically unstable although the force vanishes. This is reflected in the fact that the first non-spherical term in the site expansion of the electrostatic potential is a cubic polynomial, indicating an inflection point. The site is thus stabilized due to electronic relaxation which is accomplished by mixing of the outer alkali ions orbitals with the orbitals on its neighbors. This explains the pronounced difference between Na, for which the $2p$ orbitals are substantially more localized than the $5p$ orbitals of Cs. Note that shape of the instability or anharmonicity corresponds with the effect of the electrostatic repulsion of the four neighboring alkali ions (which form a tetrahedron), which tends to move the atom in the center away from the vertices.

In addition to the alkali ion displacement we have investigated the symmetric O mode, which corresponds to varying the internal parameter around its equilibrium value of 0.317. This Raman-active mode correspond to a simultaneous rhombohedral distortion of the OsO_6 octahedra along a cubic body diagonal (different diagonal for each of the four Os atoms in the unit cell). Locally the O atom is moving perpendicular to the line connecting its nearest-neighbor Os pair. The calculated frequency is $65 \text{ meV} = 525 \text{ cm}^{-1}$. Similar frequencies of 65 meV and 64 meV were obtained for RbOs_2O_6 and CsOs_2O_6 respectively. The deformation potential for the band crossing the Fermi level calculated at L point (very near the Fermi level) amounts to $\Delta\epsilon_k/\Delta R = 1.8 \text{ eV \AA}^{-1}$, where ΔR is the displacement of each O ion. The presence of two bands in the vicinity of the Fermi level (at the L point and close to the center of Γ -L line) makes the Fermi surface rather sensitive to this oxygen mode. These two bands move in mutually opposite directions as the oxygen is moved away from equilibrium. As a consequence displacement of the O atom by less than 0.05 \AA results in appearance of an additional electron pocket centered at the L point followed by sticking together and opening of holes along Γ -L direction in the sheets centered at Γ point.

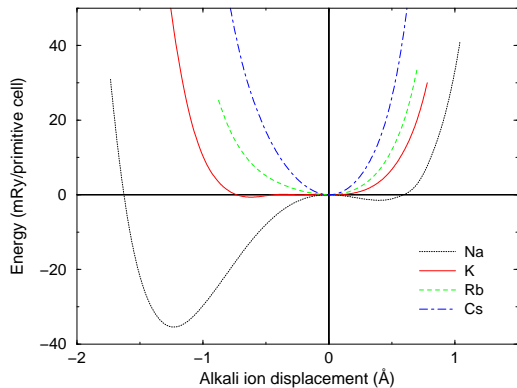


FIG. 8: (color online) Energy surface for a displacement Δ of alkali ions along $\langle 111 \rangle$ direction. The curves were obtained by spline interpolation of energies and forces evaluated at approximately ten points. Note the very large (≈ 0.5 eV) instability of the Na ion.

IV. DISCUSSION AND SUMMARY

In this paper we have analyzed the electronic structure of the β -pyrochlore KOs_2O_6 , which is nearly identical to those of the Rb and Cs compounds. The Os t_{2g} states are well separated from the more tightly bound O 2p states, and also separated from the unoccupied e_g states, leaving the focus on the complex of twelve t_{2g} -derived bands. Spin-orbit coupling has a large effect on $N(E_F)$, increasing it by 60% over its value if S-O coupling is neglected (other regions will have decreased values of $N(E)$). This system has often been compared to the other pyrochlore structure superconductor $\text{Cd}_2\text{Re}_2\text{O}_7$, which has $T_c = 1$ K. The t_{2g} bands of the two compounds have very much the same shape, with those of KOs_2O_6 being 20% wider [15]. The different band filling of these compounds precludes serious comparison of their superconducting behaviors, and the more interesting comparison is the factor of three variation in T_c within the β -pyrochlore class when they all have very similar electronic structures.

A single parameter tight binding model provides a starting point for an effective model Hamiltonian, but leaves the lower four bands flatter than observed. This aspect, as well as ordering of bands at $k=0$, can be improved by including coupling between the t_{2g} and e_g states. The calculated Fermi surfaces consist of two closed surfaces at the zone center, with flat portions, and

a large surface that is open along the $\langle 111 \rangle$ directions. The closed surfaces give rise to nesting features at specific values of q along the $\langle 110 \rangle$ direction, but while sharp the features are not very strong.

Investigation of the strength of electronic correlations has been initiated here. Comparison of the measured linear specific heat coefficient γ for RbOs_2O_6 with the calculated value of $N(E_F)$ leads to a dynamic quasiparticle mass enhancement $\lambda = 2.4$, indicating important correlation effects but far from heavy fermion type of behavior. Calculation of the Stoner enhancement of the $q=0$ susceptibility gives a factor of two, again indicating important correlation corrections but nothing close to a ferromagnetic instability.

The only substantial difference between the K, Rb, and Cs compounds that we have found is the degree of (in)stability of the alkali cation in its tetrahedral interstitial site. The potential for K ion motion along the $\langle 111 \rangle$ directions is flat over a distance of almost 1 Å, indicating an extremely floppy ion whose motion may provide the scattering of carriers that is reflected in peculiar concave-downward resistivity at low temperature. The Rb and Cs ions are progressively more stable, and their resistivity behavior is more conventional. Calculation for the Na compound (not yet reported) indicates a seriously unstable potential surface, with the minimum being more than 1 Å away from the normal high symmetry site of the cation. This instability may make the Na compounds unstable (and unsynthesizable) in this structure.

The close similarity of the electronic structures of the compounds in the KOs_2O_6 series, as well as almost identical equilibrium position and dynamics of the O ion, allows two explanations of the largely different T_c 's: (i) fine details of the electronic structure at the Fermi level are very important, (ii) the very different degree of anharmonicity of the alkali ion is responsible for the differences in T_c . We propose that the pressure dependence of T_c can resolve these two scenarios. In scenario (i) a strong pressure dependence of T_c with a negative slope is expected following the trend across the K-Rb-Cs series. On the other hand the alkali ion dynamics, determined primarily by its ionic radius, is not sensitive to small changes of the volume and so no dramatic pressure dependence of T_c is expected if scenario (ii) applies.

J. K. was supported by DOE grant DE-FG03-01ER45876, while W. E. P. was supported by NSF Grant DMR-0421810.

-
- [1] A. P. Ramirez, *Annu. Rev. Mater. Sci.* **24**, 453 (1994).
 - [2] B. Canals and C. Lacroix, *Phys. Rev. B* **61**, 1149 (2000).
 - [3] S. Yonezawa, Y. Muraoka, Y. Matsushita, and Z. Hiroi, *J. Phys. Condens. Matter* **16**, L9 (2004).
 - [4] Z. Hiroi, S. Yonezawa and Y. Muraoka, *J. Phys. Soc. Japan* **73**, 1651 (2004).
 - [5] S. Yonezawa, Y. Muraoka, Y. Matsushita, and Z. Hiroi, *J.*

- Phys. Soc. Jan.* **73**, 819 (2004).
- [6] S. Yonezawa, Y. Muraoka, and Z. Hiroi, *cond-mat/0404220*.
- [7] S. Hanawa, Y. Muraoka, T. Tayama, T. Sakakibara, J. Yamaura, and Z. Hiroi, *Phys. Rev. Lett.* **87**, 187001 (2001); R. Jin, J. He, S. McCall, C. S. Alexander, F. Drymiotis, and D. Mandrus, *Phys. Rev. B* **64** 180503

- (2001).
- [8] M. Brühwiler, S. M. Kazakov, N. D. Zhigadlo, J. Karpinski, and B. Batlogg, Phys. Rev. B **70**, 020503 (2004).
- [9] K. Koepf, and H. Eschrig, Phys. Rev. B **59**, 1743 (1999); H. Eschrig, *Optimized LCAO Method and the Electronic Structure of Extended Systems* (Springer, Berlin, 1989).
- [10] P. Blaha, K. Schwarz, G. K. H. Madsen, D. Kvasnicka, and J. Luitz, Wien2k, *An Augmented Plane Wave + Local Orbitals Program for Calculating Crystal Properties* (Karlheinz Schwarz, Techn. Universität Wien, Wien, 2001), ISBN 3-9501031-1-2.
- [11] J. P. Perdew and Y. Wang, Phys. Rev. B **45**, 13244 (1992).
- [12] S. Fujimoto, Phys. Rev. B **64**, 085102 (2001).
- [13] D. J. Singh, P. Blaha, K. Schwarz, and I. I. Mazin, Phys. Rev. B **60**, 16359 (1999).
- [14] J. F. Janak, Phys. Rev. B **16**, 255 (1977); S. H. Vosko and J. P. Perdew, Can. J. Phys. **53**, 1385 (1975)
- [15] D. J. Singh, P. Blaha, K. Schwarz, and J. O. Sofo, Phys. Rev. B **65**, 155109 (2002)